International Journal of Mechanical Engineering and Technology (IJMET)
Volume 9, Issue 8, August 2018, pp. 9–23, Article ID: IJMET_09_08_002
Available online at http://www.iaeme.com/ijmet/issues.asp?JType=IJMET&VType=9&IType=8
ISSN Print: 0976-6340 and ISSN Online: 0976-6359

WEAR AND CORROSION RESISTANCE OF EXCAVATOR SHOE BEFORE AND AFTER HEAT TREATMENT

Sumar Hadi Suryo, A. P. Bayuseno, Yurianto, Moch and Fihki Fachrizal
Department of Mechanical Engineering, University of Diponegoro, Semarang, Indonesia,
Prof. Sudharto, SH. Street, Tembalang, Semarang 50275

ABSTRACT

An Excavator is heavy equipment used in construction, agriculture and forestry industries. An Excavator has a primary function of digging and loading materials, such as rocky soils and others. An Excavator has three (3) sections consisting of an attachment, a base frame, and the undercarriage. One section of the undercarriage in an excavator that constantly needs routine maintenance is the track shoe. A Track shoe is the crawler or the outer wheel of an excavator that serves as the motor of the excavator. This section is always in direct contact with the soil which leads to wear. This research discusses the comparison of medium properties of the shoe material before and after heat treatment using quenching with oil media. The material used was AISI 1526. The analysis conducted was a micrographic test in which non-heat-treatment material underwent ferrite and pearlite phases, while the heat-treatment material turned into a martensite phase. Microstructure testing of the sample was conducted using optical microscope. The hardness testing of the sample used Rockwell Hardness Tester, while the wear testing used Ogoshi High Speed Universal Wear Method, and corrosion testing used potentiodynamic polarization method. From the analysis results, hardness value was inversely proportional to wear and corrosion values; the harder the material, the smaller the wear rate.

Keywords: AISI 1526, track shoe, excavator, microstructure, wear testing, hardness testing, corrosion testing, Ogoshi High Speed Universal Wear, potentiodynamic polarization
Cite this Article: Sumar Hadi Suryo, A. P. Bayuseno, YuriantoParyanto and Moch. Fihki Fachrizal, Wear and Corrosion Resistance of Excavator Shoe Before and After Heat Treatment, International Journal of Mechanical Engineering and Technology, 9(8), 2018, pp. 9–23.
http://www.iaeme.com/IJMET/issues.asp?JType=IJMET&VType=9&IType=8

1. INTRODUCTION

Technological development increases rapidly from time to time. In addition, one of technologies that have rapid development is the technology of heavy equipment industry. It is because the use of heavy equipment is increasingly vital in the development of industrial world, such as mining, property, infrastructure and others. Particularly, there are several types of heavy equipment, depending on the function, one of which is the excavator unit (Indonesian Ministry of Public Works, 2012). Excavator takes the biggest role in the heavy equipment industry from all sectors. Based on the data from the Ministry of Public Works from 2013 to 2020, the need for heavy equipment is very high compared to the availability of heavy equipment itself. Therefore, it can be concluded that heavy equipment is vital in national development and the most widely used weight heavy equipment is excavator. It can be seen in Figure 1.

Figure 1 Diagram of comparison of the use of heavy equipment in Indonesia (Indonesian Ministry of Public Works, 2012).

Excavator is heavy equipment that is used in construction, agriculture or forestry industries. Excavator has a primary function for digging and loading materials such as soil and rocks into the truck or congested location. Excavator has several sections including attachment, base frame and undercarriage. Undercarriage is one of the most common motor tools in construction machinery that serve to move the excavator forward, backward, left and right. Undercarriage works in a system. High mobility in severe field condition can lead to damage to the vital part of the motor in the excavator; it is the chain link (Bošnjak et al., 2013). Chain link is a major component of undercarriage (Ryu et al., 2000; Rubinstein & Coppock, 2007). Wear or damage to chain link components mostly is due to the magnitude of the force that occurs in the excavator during the operating activity and the material strength values that are less suitable for the field (Bošnjak et al., 2011; Dudek et al., 2011).

Undercarriage consists of several sections, one of which is the excavator crawler. Crawler or excavator track shoe is the wheel of excavator, some have wheels of ordinary tires used for dense and flat streets called “Wheel Excavators” and some have wheels of chains iron that will make it easier to pass on the streets that are not dense or uphill. This chains-iron wheel excavator is also called “Crawler Excavators”. Most of excavators work on soft ground soil. Therefore, based on the experience, it causes problems to the track shoe. If the track shoe always works on harsh conditions, then the damage to the bottom part (track shoe) will be very soon, so in the selection of excavator, track shoe factor must be noticed and considered (Prasetya & Krisnaputra, 2014).

Track Shoe is the outermost part of the undercarriage that serves as the "wheel" of the excavator. Section of track shoe is divided into 3 types: triple grouser section, double grouser section and single grouser section. Track shoe is designed in such a way to be able to withstand the load from the excavator and to withstand the force of the ground while running on it (United Tractors School, 2008).

Track Shoe must have good usage to materials such as wet soil and rocks as well as to terrains that have abrasive properties caused by the nature of the soil when the track shoe crushes the material. John Deere (2007) mentioned that 50% of the largest maintenance cost on excavator is on the undercarriage. In addition, track shoe is one section of the

undercarriage that needs more attention because this section is always in direct contact with the ground.

Maulana et al. (2017) conducted a research on the damage analysis of undercarriage components of Hitachi EX200 excavator using FMEA method. Based on the results of the research, it can be seen that the track shoe becomes one section of undercarriage which has the second highest RPN percentage of experiencing failure after sprocket.

Based on the previous research, it can be concluded that most arising problem on the excavator is on the track shoe. Therefore, the authors examine the excavator track shoe by comparing the metallic properties that have different characteristics due to heat treatment, examining the value of track shoe wear using Ogoshi High Speed Universal Wear method and examining the value of corrosivity rate using potentiodynamic polarization method. Thus, it requires a special handling so that each element of the metal can be used as what is expected.

2. LITERATURE REVIEW

2.1. Definition of Track Shoe

The track shoe is a component or section of the undercarriage which functions at the point of contact with the ground and is driven by the excavator crawler's motor. The track shoe sections serve to sustain the weight of the equipment and pass the load to the surface of the ground, which could be hard or soft. In addition, the track shoe, in conjunction with the steering and brake systems, moves and controls the excavator. The track shoe is mounted on the excavator, enabling operation of the equipment even in rocky areas. In comparison with operations in a sandy area, the wear rate of the track shoe tends to be greater in such areas. The track shoe is equipped with a rib that helps to reduce lateral friction, and it is also equipped with a bolt guard intended to reduce damage to the head of the bolt. The various types of excavator track are shown in Table 1.

Table 1 Kinds of excavator track shoe (Komatsu, 2009)

Kinds of Track Shoe	Description	Figure
Single Grouser Shoe	Provides great traction, is designed for rugged and rocky operation areas and is commonly used for straight dozers and angle dozers.	
Double Grouser Shoe	Used to provide excellent traction with a short turning radius.	
Triple Grouser Shoe	Commonly used for dozer shovels and excavators, provides less traction but high maneuverability and is efficient when operated on soft soil.	
Flat Shoe	Used in the operation on asphalt roads to minimize road damage, has no traction which allows for slippage during operations.	

Swamp Shoe	Triangle shaped so the contact section with the ground is wider, used in muddy areas.	
Rubber Shoe	Only used when the tractor (bulldozer or dozer shovel) runs on the highway so as not to damage the surface of the asphalt road.	

Most excavators work on a variety of surfaces ranging from hard pavement to soft soil. Experience shows each of these surfaces can potentially cause problems for the track shoe. If the track shoe is always used in areas with hard surfaces and difficult conditions, then damage to the bottom sections of the track shoe may occur very rapidly. For general use, the "triple grouser section" type of shoe (a wheel with three layers/sections) is recommended because it maintains good traction while also doing minimal damage to the surface (Rochmanhadi, 1992). For all of the tests conducted in this research, the type of track shoe used is the triple grouser shoe with a 20 ton capacity.

2.2. Wear

Maulana et al. (2017) conducted research analysing damage to undercarriage components on the Hitachi EX200 excavator using the FMEA method. Based on the results of the research, the track shoe has been determined to be a section of the undercarriage which is quite vulnerable to damage. Therefore, the track shoe should receive careful consideration in terms of selection, installation and maintenance practices.

Wear is generally defined as the progressive loss of material from a component or the transfer of material from one surface to another as a result of the relative movement or friction between the two surfaces. Wear has been a practical concern for a long time but has not been well-researched in terms of scientific explanations or the mechanism of damages related to tensile strength, impact, tipple or fatigue loading. Discussion of the mechanism of wear on any material is closely related to friction and lubrication. Research on these three subjects is known as Tribology. Wear is not a basic property of a particular material; rather, it is the material's response to an outer system (surface contact). Any material can experience wear due to various mechanisms.

Wear testing can be conducted using various methods and techniques, all of which aim to simulate actual wear conditions. One method is known as the Ogoshi method, in which the specimen obtains a frictional load from a revolving disc. This frictional loading results in repeated surface-to-surface contact which will eventually transfer some of the material from the surface of the specimen. The magnitude of the surface traces of the frictional material is the basis for determining the level of wear on the material; the larger and deeper the wear, the higher the volume of peeling material from the specimen (Ogoshi High Speed Universal Wear Testing Instruction Manual).

Any type of material will experience adhesive wear, abrasive wear, erosion wear and oxidation wear. The following is a brief description of the mechanisms (Dasgubta et al., 1998):

1. Adhesive Wear

This occurs when the surface contact of two or more materials results in attachment to each other (adhesive) and plastic deformation which finally leads to the release of one of the materials (Dasgubta et al., 1998).

2. Abrasive Wear

This occurs when hard particles (asperity) from a particular material slide along the surface of another, softer material, resulting in penetration or cutting of the softer material (Dasgubta et al., 1998).

3. Erosion Wear

The process of erosion is caused by gases and liquids carrying solid particles which strike on the surface of the material. If the impact angle is small, the wear is analogous to abrasive wear. However, if the impact angle forms a normal force angle of 90°, then wear will result in a brittle failure of its surface.

4. Oxidation/Corrosive Wear

This type of damage begins with a chemical change in the surface of the material caused by environmental factors. Contact with the environment results in the formation of superficial layers with different properties from the parent material. As a consequence, the degradation of the material leads to interface fractures between the surface layer and the parent material, and eventually the entire surface layer will be displaced (John Deere, 2007).

3. RESEARCH METHOD

In the first stage of the experiment, the tools and materials were prepared. The track shoe material (AISI 1526) was cut into a number of equivalent specimens. The second stage involved a heat treatment process, heating a specimen up to 885°C, followed by quick cooling (quenching) using oil media. Each heat-treated specimen then was examined to determine whether it was viable to continue to be used for the next stage. Once each sample of material was determined to be viable, it underwent a laboratory testing process in order to measure specific characteristics. This laboratory testing included composition testing, hardness testing, microstructure testing, wear testing and corrosion testing.

3.1. Chemical composition evaluation

Composition testing results identified the various elements which composed the specimen. Next, determining the percentage of carbon was useful to determine the temperature of austenite during the heat treatment process. In addition, the results of composition testing were used to calculate the corrosion rate.

3.2. Hardness Testing

Hardness testing enabled the researchers to determine the level of hardness in each specimen. This study used the Rockwell hardness method, using a Rockwell Hardness Tester in C-scale (HRC) where the scale used 150 kgf loading with a penetrator diamond cone (ASTM E18 – 3). The testing was conducted comparing heat-treated and non-heat-treated specimens and each specimen was tested at 3 different points.

3.3. Microstructure examination

Microstructure testing analyzed the results of heat treatment on the components of the track shoe. This test used the Olympus brand BX41M microscope with 200x magnification. The specimens for microstructure testing were prepared by first undergoing a polishing process using sandpaper and autosol, then etching with a solution of 2.5 ml HNO_3, 1ml HF, 1.5ml HCl, and 95 ml of Aquades.

3.4. Wear Testing

Wear is the loss of material from a surface, or transfer of material from its surface to another part, or the movement of material to a surface (Almen, 1950). Wear caused by mechanical behavior is reclassified into abrasive, adhesive, flow and fatigue wear. In the wear testing for this research, the wear type studied was abrasive wear. Abrasive wear in earth moving equipment occurs when hard particles or rough hard surfaces crush and cut off a softer surface, resulting in loss of the material from the original surface (Zum Gahr, 1987). This test was carried out using an Ogoshi Universal High Speed Testing Machine, in which the specimen experienced friction by undergoing loading from a rotating ring, with wear duration of 1 minute. This frictional loading intensified with repetitive contact between the two surfaces, which eventually caused some of the material to be removed from the sample surface and deposited on the other. The magnitude of the surface traces of the frictional material is the basis for determining the level of material wear.

The calculation of wear rate uses the formula of Archad's Law (1953). In order to calculate correctly, it is necessary to know the specific value of the abrasive, using the following formula:

$$Ws = \frac{B.bo^3}{8.r.Po.lo} \quad (1)$$

Ws is the specific wear rate (mm^2/kg); B is the thickness of the disc (mm); Bo is the area of the abrasive material (mm)*;* r is the radius of the disc (mm); Po is the load value (kg)*;* and Lo is the abrasion distance (m) (Ogoshi High Speed Universal Wear Testing Machine Instruction Manual).

The calculation for the rate of wear uses Archad's Law:

$$V = K_D \times F \times s \quad (2)$$

V is the lost material volume due to wear; K_D is the wear coefficient or specific abrasion; F is the reaction force of the component or material; and s is the length/distance where the components are sliding against each other (*sliding distance*) (Dasgubta et al., 1998).

3.5. Corrosion Testing

The testing process was conducted using the potentiodynamic polarization method; in this method, the amount of corrosion of the metal is determined based on potential and anodic or cathodic currents. Metal corrosion has occurred when the anodic current was equal to the cathodic current even though there was no current provided outside the system, due to the difference in potential between the metal and the solution, which is the environment (Sunarya, 2008). The corrosion rate can be determined by this method using a three-electrode potentiometer; it consists of a saturated calomel electrode (SCE), an auxiliary electrode formed of platinum, and a working electrode formed of the steel in the specimen. The data obtained from this method was plotted as an anodic/cathodic polarization curve which states the relationship between the current ($\mu A / cm^2$) as a potential function (mV).

The corrosion rate testing was conducted by observing the intensity of the corrosion current (Icorr) of the specimen in a Sodium Chloride (NaCl) environment. The determination of Icorr was crucial because Icorr is directly proportional to the magnitude of the corrosion rate of a metal in its environment. The calculations to determine the corrosion rate in this experiment use a method based on the potential curve vs. intensity log of corrosion current.

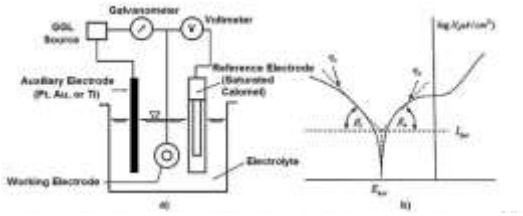

Figure 2 a) Scheme of corrosion tester with the type of three-electrode cell, b) the polarization curve (Tretheway & Chamberlain, 1991).

The corrosion current density (Icorr) is obtained from the potential curve logarithm of the current intensity curve by determining the intersection point of the reduction reaction Tafel line (η_c) and the oxidation reaction Tafel line (η_a) on the logarithm line of the current intensity by determining the intersection point of the reduction reaction Tafel line (η_c) and the oxidation reaction Tafel line (η_a) on the corrosion potential line. The values of η_c and η_a were determined by the following equation (Jones, 1992):

$$\eta_a = \beta_a log \frac{i_a}{i_0} \quad 3$$

$$\eta_c = \beta_c log \frac{i_c}{i_0} \quad 4$$

η_a is the oxidation reaction Tafel; η_c is the reduction reaction Tafel; i_a is the current at the anode reaction; i_c is the current at the cathode reaction; i_0 is the current at the change of reduction to the oxidation reaction; β_c is the Tafel gradient of cathode reaction; and β_a is the Tafel gradient of anode reaction

The value of the corrosion rate can be determined based on the value of the corrosion current density in which the value of the corrosion rate of a metal in its environment is equal to the value of the corrosion current density. It is based on the corrosion rate equation (Jones, 1992) as follows:

$$r = 0{,}129 \frac{ai}{nD} \quad 5$$

r is the corrosion rate (mpy); a is the atomic mass number or atomic weight; i is the corrosion current density ($\mu A/cm^2$); n is the atomic valence; and D is the specimen density (gr/cm^3).

Comparison of the corrosion rate to be combined is initially calculated by equivalent weight with the following equation (Möller, 2006):

$$EW = N_{EQ}^{-1} \quad 6$$

$$N_{EQ} = \sum \left(\frac{\omega_i}{a_i/n_i} \right) = \sum \left(\frac{\omega_i n_i}{a_i} \right) \quad 7$$

EW is the equivalent weight; N_{EQ} is the total equivalent value; ω_i is the atomic weight fraction; a_i is the atomic mass number; and n_i is the atomic valence electron. The equation for the corrosion rate becomes the following equation:

$$r = 0{,}129 \frac{i_{corr}(EW)}{D} \quad 8$$

The result of the above corrosion rate equations are still in mpy (mils per year). To change the unit, the following conversion of mpy to the matrix unit is required.

$$1mpy = 0{,}0254 \frac{mm}{yr} = 25{,}4 \frac{\mu m}{yr} = 2{,}899 \frac{nm}{hr} = 0{,}805 \frac{pm}{sec}$$

By looking at the comparison table of mpy with other matrix units against the corrosion rate in D. A. Jones "Principles and Prevention of Corrosion" book in 1992, we can determine the corrosion rate of the material, as shown in Table 2.

Table 2 Comparison of mpy with other matrix units against corrosion rate

RCR	mpy	mm/yr	µm/yr	nm/h	pm/s
Outstanding	< 1	< 0.02	< 25	< 2	< 1
Excellent	1 – 5	0.02 – 0.1	25 – 100	2 – 10	1 – 5
Good	5 – 20	0.1 – 0.5	100 – 500	10 – 50	20 – 50
Fair	20 – 50	0.5 – 1	500 – 1000	50 – 150	20 – 50
Poor	50 – 200	1 – 5	1000 – 5000	150 – 500	50 – 200
Unacceptable	200+	5+	5000+	500+	200+

4. RESULTS AND DISCUSSION

4.1. Track Shoe Modeling

The modeling was made on a 1: 1 scale with the actual size. Dimensional data such as length, width and height were generated by reference to the size of the track shoe dimensions that were obtained from field measurements and Komatsu catalogs. The data obtained were sufficient to meet the parameters that will be the size of the track shoe using AISI 1526 steel material.

Based on the specifications, a model of the track shoe can be made using CAD software. The CAD software used for this modeling is Solid Works 2016 and results can be seen in Figure 3.

Figure 3 3-dimensional modeling of track shoe

The track shoe dimensions from the top and side specifications are shown in Figure 2.

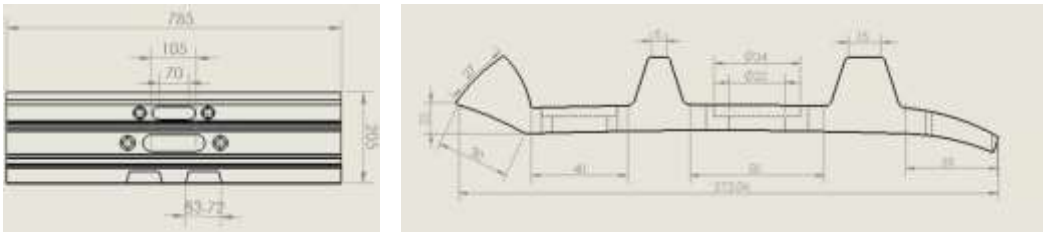

(a) (b)

Figure 4 Size of track shoe dimensions from the top (a) and side (b) specifications.

The material that was tested consisted of AISI 1526 standard combination steel and the figures were designed using Solid Works 2016 software.

4.2. The Results of Chemical Composition Testing

Table 3 The Results of Chemical Composition Testing

No.	Element	Percentage of Content (%)	No.	Element	Percentage of Content (%)
1.	C	0.2665	13.	Al	0.0011
2.	Si	0.2667	14.	Nb	0.003
3.	S	0.0115	15.	V	0.0037
4.	P	0.0164	16.	Co	0.0000
5.	Mn	1.2427	17.	Pb	0.0012
6.	Ni	0.0280	18.	Ca	0.000
7.	Cr	0.3853	19.	Zn	97.5969
8.	Mo	0.0010	20.	Fe	0.0024
9.	Cu	0.0639	21.	O	0.0150
10.	W	0.0020	22.	N	0.0039
11.	Ti	0.0463	23.	Sb	0.0011
12.	Sn	0.0006			

From chemical composition testing, the bucket teeth material that underwent the treatment process, including medium carbon steel, had approximately 0.26% carbon content.

4.3. The Result of Hardness Testing

Hardness testing for this research was conducted using the Rockwell Hardness Tester tool, which uses C-Scale (HRC) with 150 Kgf loading and the use of a diamond cone. The testing was conducted on the surface of the specimen. Each specimen had 3 (three) tests as shown in Figure 5.

Figure 5 The specimen of hardness testing

Table 4 Hardness value without heat treatment (left) and with heat treatment (right) (HRC Scale)

Point	Untreated Specimen (HRC)	Point	Specimen of quenching with oil media
1	42	1	45
2	40	2	44
3	41	3	47
Average	41	Average	45.3

Based on Table 4, we can draw a comparison chart as shown in Figure 6.

Figure 6 Chart of hardness value

Based on the chart, it can be seen that the specimen that underwent heat treatment with oil media quenching has a higher hardness value compared with the specimen that was not heat treated. This increased hardness value occurred only on the surface of the specimen because the specimen was only heated on its surface. The highest hardness value is at point 3, at the front point of the specimen, with a hardness value of 47 HRC, followed by points 1 and 2 (located on the left and center sides respectively), with a hardness value at point 1 of 45 HRC and at point 2 of 44 HRC. The values differed at each point due to the variations in the effects of the heat treatment; because the heat treatment process only affected the surface of the material, the heating was uneven.

4.4. The Result of Microstructure Testing

Microstructure testing was conducted on specimens that did not undergo the heat treatment process, and on those that used water as a quench medium.

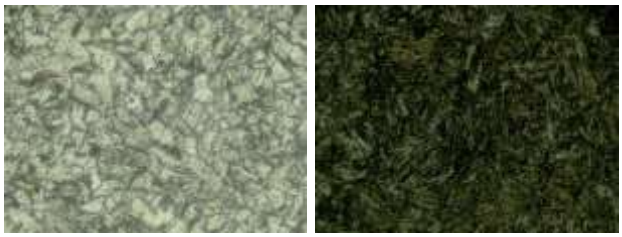

(a) (b)

Figure 7 The results of microstructure testing on the specimen (a) untreated (b) oil quenched

From Figure 7a, the microstructure of the material before undergoing heat treatment indicates ferrite and pearlite phases while Figure 7b shows that the microstructure of the material after oil quenching formed the martensite phase. This takes place because a rapid cooling process with higher heating temperatures results in the martensite phase. When the sample was heated, the grains of the pearlite and ferrite phases grew larger.

4.5. The Result of Wear Testing

This wear testing was designed to determine the specific amount of wear, with wear value stated in mm^2/kg. In this study, the test used the Ogoshi Universal High Speed Testing method in which the specimen was sliding with a load of 19.08 kg from the rotating ring for a 1-minute duration. This frictional loading result in repeated contact between surfaces and eventually the surface of the specimen will take some of the material on its surface. The magnitude of the surface traces of the sliding specimens was the basis for determining the wear rate of the material (Sarkar, 1980).

Following are the results of the data from wear testing using the Ogoshi Universal High Speed Testing method.

Figure 8 The specimen for wear testing.

Table 5 Testing value of wear area without heat treatment and with heat treatment.

Treatment	Point	Number of Scratches					Average Area	*bo* (mm)
Without heat treatment	1	20	27	38	21	25	26.2	0.68947
	2	19	30	30	20	28	25.4	0.66842
	3	18	37	30	28	27	28	0.73684
With heat treatment	1	25	19	27	22	28	24.2	0.63684
	2	28	22	25	20	31	25.2	0.66315
	3	28	24	31	22	29	26.8	0.70526

The calculation sample for determining the value of *bo* (mm) is at point 2 for an untreated specimen in which each magnification 100x = 38 strip = 1 mm (Ogoshi High Speed Instruction Manual).

$$bo = \frac{\sum \text{area}}{38\ strip}$$

$$bo = \frac{25{,}4}{38}$$

$$bo = 0{,}66842 \text{ mm}$$

After obtaining the value of *bo*, the value is then inserted into the formula to determine the sample's specific wear value; following is the formula (Ogoshi High Speed Instruction Manual):

$$\text{Ws} = \frac{\text{B}.bo^3}{8.\text{r.Po.Lo}} \quad (9)$$

Ws = wear specific value (mm^2/kg)

B = wear disc thickness (mm)

bo = the width of the wear of the specimen (mm)

Po = load during wear testing (kg)

Lo = distance during wear process (m)

The sample calculation of one point (point 2) that has been known is:

B = 3 mm

r = 15 mm

Po = 6.36 kg

Lo = 200 m = 200000 mm

$$Ws = \frac{3 \text{ mm} \times (0.67)^3}{8 \times 15 \text{ mm} \times 6{,}36 \text{ kg} \times 200000 \text{ mm}}$$

$$Ws = 5{,}91 \times 10^{-9} \text{ mm}^2/\text{kg}$$

Table 6 The value of wear testing without heat treatment and with heat treatment.

Treatment	Point	*bo* (mm)	bo^3 (mm)	Ws (mm^2/kg)
Without heat treatment	1	0.69	0.328509	6.46 x 10^{-9}
	2	0.67	0.300763	5.91 x 10^{-9}
	3	0.74	0.405224	7.96 x 10^{-9}
With heat treatment	1	0.64	0.262144	5.15 x 10^{-9}
	2	0.66	0.287496	5.65 x 10^{-9}
	3	0.71	0.35791	7.03 x 10^{-9}

Further explanation of the data is shown in the chart which is shown in Figure 9.

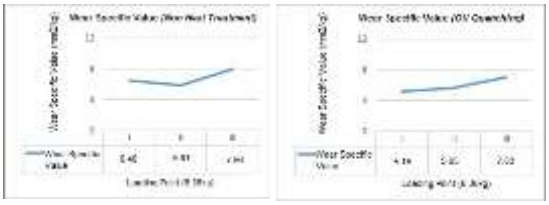

(a) (b)

Figure 9 Chart of abrasive specific values (a) untreated (b) oil quenched.

To find the predicted wear rate that will occur on the excavator track shoe Archard's law can be used:

Archard Wear Volume $V = K_D \times F \times s$

V = the lost material volume due to the wear

K_D = wear coefficient of specific abrasion

F = reaction forces on components or materials

s = the distance when the components are sliding (sliding distance)

After determining the calculation for specific abrasion, the lowest value was taken from each specimen; untreated was 5.91 x 10^{-9} mm^2/kg and oil quenched was 5.15 x 10^{-9}.

The calculation:

K_D = Untreated (5.91 x 10^{-9} mm^2/kg); Oil Quenched (5.15 x 10^{-9})

F = 17.300 kg *(*Traction Force*)* Source: Catalogue Hitachi

s = 12.546 $\frac{m}{day}$ = 12.546.000 $\frac{mm}{day}$

For Untreated

V = 5.91 x 10^{-9} mm^2/kg x 17.300 kg x 12.546.000 $\frac{mm}{day}$

V = 1.28 $\frac{mm^3}{day}$

For Oil Quenched

V = 5.15 x 10^{-9} mm^2/kg x 17.300 kg x 12.546.000 $\frac{mm}{day}$

V = 1.12 $\frac{mm^3}{day}$

4.6. The Result of Corrosion Testing

This corrosion test was designed to determine the magnitude of the corrosion rate value, stated in units of mpy (mils per year). In this study, the test used the Potentiodynamic Polarization method. The specimen was inserted into the holder and immersed into the electrolyte solution in the reaction flask tube. The electrolyte solution was composed of 2.98% NaCl based on the data of the NaCl solution content at Tanjung Mas Semarang Port (Ispandriatno & Krisnaputra, 2015)

The following is the result of the data from corrosion rate testing using the Potentiodynamic Polarization method in Table 7.

Table 7 The value *Icorrosion* for Untreated and Quenched Air materials.

Icorrosion	
Untreated	Water Quenched
48.232 µA	32.163 µA

To calculate combined corrosion rate, initially the equivalent weight (Equivalent Weight = EW) must be determined using the following equation:

$EW = N_{EQ}^{-1}$

$$N_{EQ}^{-1} = \sum \left[\frac{\omega_i}{a_i/n_i}\right] = \sum \left[\frac{\omega_i n_i}{a_i}\right] \quad 10$$

Description:

EW = equivalent weight

N_{EQ} = the value of total equivalent

ω_i = weight fraction of atom i

a_i = mass number of atom i

n_i = valence electron of atom i

The weight fraction of an atom can be found in Table 3, which is the result of AISI 1526 composition testing. The mass number of an atom can be found in the periodic table and the results can be seen in Table 8.

Table 8 The mass value of the atom.

Fe = 55.845	S = 32.065	Al = 26.982	C = 12.011	Ni = 58.693
Nb = 92.906	Si = 28.086	Cr = 51.996	V = 50.942	Mn = 59.938
Mo = 95.94	W = 183.84	P = 30.974	Cu = 63.546	Ti = 47.867
N = 14.007	B = 10.811	So = 121.76	Ca = 40.078	Mg = 24.305
Zn = 65.38	Co = 58.933	Pb = 207.2		

The valence electron values for all elements can be seen in Table 9.

Table 9 Valence electron value

C = 4	Si = 4	Pb = 4	Al = 3	S = 6
P = 5	N = 5	B = 3	Sb = 5	Ca = 2
Mg = 2	Fe = 2	Ni = 2	Nb = 2	Cr = 1
V = 2	Mn = 2	Mo = 2	W = 2	Cu = 1
Ti = 2	Zn = 2	Co = 2		

After obtaining the value of the fraction weight of an atom, the atomic mass and valence electron, then we look for the value of EQ (Equivalent total) and analyze the sample using the value for the element Iron (Fe) (Jones, 1992).

$$N_{EQ}^{-1} = \sum \left[\frac{\omega_i}{a_i/n_i}\right] = \sum \left[\frac{\omega_i n_i}{a_i}\right]$$

$$Fe = \left(\frac{0{,}975969\ x\ 2}{55{,}845}\right) = 0.0349527$$

Table 10 EQ Value (Total Equivalent)

C = 0.0008875	Si = 0.0003812	Pb = 0	Al = 0.0000375	S = 0.0000215
P = 0.0000265	N = 0.0000535	B = 0.0000067	Sb = 0.0000016	Ca = 0.0000006
Mg = 0.000006	Fe = 0.0349527	Ni = 0.0000095	Nb = 0.00000023	Cr = 0.0000741
V = 0.0000012	Mn = 0.0004524	Mo = 0.0000044	W = 0.00000022	Cu = 0.00001
Ti = 0.0000193	Zn = 0.0000002	Co = 0.0000013		

$\sum EQ = 0.04036961$

$EW = N_{EQ}^{-1}$

$= 0.09036961^{-1}$

$= 24.771$

To find the value for the corrosion rate, the equation is:

Icorr (Not Heat Treated) = 48.232µA

Icorr (Oil Quenched) = 32.163 µA

$$r = 0.129\ \frac{i_{corr}(EW)}{D}$$

- Non Heat Treatment = $0.129\ x\ \frac{48.232\ x\ (24.771)}{7.7}$ = 20.02 mpy
- Oil Quenched = $0.129\ x\ \frac{32.163\ x\ (24.771)}{7.7}$ = 13.34 mpy

The conversion of mils per year to matrix units:

$$1mpy = 0.0254\frac{mm}{yr} = 25.4\ \frac{\mu m}{yr} = 2.899\ \frac{nm}{hr} = 0.805\ \frac{pm}{sec}$$

Therefore,

- Non Heat Treatment whose value is 20,02 *mpy* = 0,51 $\frac{mm}{yr}$
- Water Quenched whose value is 13,34 *mpy* = 0,34 $\frac{mm}{yr}$

Thus, we can determine the material properties of the corrosion rate. AISI 1526 un-treated has a corrosion rate value of 0.51 $\frac{mm}{yr}$ which is classified as Fair in the table; i.e. between 0.5 - 1 $\frac{mm}{yr}$. Meanwhile, the results for AISI 1526 quenched with oil medium indicates a corrosion rate value of 0.34 $\frac{mm}{yr}$ which is classified as Good in the table; i.e. between 0.5 - 1 $\frac{mm}{yr}$. It can be concluded that AISI 1526 material with oil media quenching has better corrosion resistance than untreated AISI 1526 material.

5. CONCLUSIONS

Based on the research that has been conducted, some conclusions can be drawn as follows:

1. Results of Hardness Testing
2. The results of hardness testing returned a value for non-heat-treated material of 41 HRC, while the material of heat treatment with oil quenching was 45.3 HRC, so it can be concluded that the process of heat treatment quenched with oil media can increase the hardness value of the material.
3. The Result of Microstructure Testing
4. Based on the results of microstructure testing, untreated material went to the ferrite and pearlite phases while the material which underwent the oil quenching process went to the martensite phase, which proves that the heat-treated, oil-quenched material was harder than untreated material.
5. The Result of Wear Testing Using the Ogoshi Universal High Speed Testing Method
6. From the results of wear testing, the wear rate of non-heat-treatment material was determined to be 1.28mm^3/day and the material using heat treatment with oil quenching was determined to be only 1.12mm^3/day. Because the value for the oil quenched sample was smaller than the untreated value, it has been shown that the oil-quenched specimen was more resistant to wear.
7. The Result of Corrosion Testing Using the Potentiodynamic Polarization Method
8. Based on the result of corrosion testing, the wear rate of heat-treatment material was 0.51 mm/yr and untreated material was 0.34 mm/yr, so the corrosion rate for

untreated material was considered to be Fair and the material with oil quenching was considered to be Good.

REFERENCES

[1] Almen, J.O. 1950. In Mechanical Wear (ed J.T. Burwell). Amarican Society for Metals. 229-288.

[2] ASTM E18 – 3, Standard Test Methods for Rockwell Hardness and Rockwell Superficial Hardness of Metallic Materials.

[3] Bošnjak, S.M., Arsic, M.A., Zrnic, N.D., Odanovic, Z.D., and Dordevic, M.D. 2011. Failure analysis of the stacker crawler chain link. Procedia Engineering. 10: 2244-2249.

[4] Bošnjak, S.M., Momčilović, D.B., Petković, Z.D., Pantelić, M.P., and Gnjatović, N.B. 2013. Failure investigation of the bucket wheel excavator crawler chain link. Engineering Failure Analysis. 15(35): 462-469.

[5] Dasgubta, R., Prasad, B.K., Jha, A.K., Modi,O.P., Das, S., and Yegneswaran, A.H. 1998. Low stress abrasive wear behavior of a hardfaced steel. Journal of Materials Engineering and Performance. 7(2): 221-226.

[6] Dudek, D., Frydman, S., Huss, W., and Peogo, G. 2011. The L35GSM cast steel–possibilities of structure and properties shaping at the example of crawler links. Archives of Civil and Mechanical Engineering. 11(1): 19-32.

[7] Ispandriatno, A.S., and Krisnaputra, R. 2015. Ketahanan Korosi Baja Ringan di Lingkungan Air Laut. Jurnal Material dan Teknologi Proses, 1(1).

[8] John Deere. 2007. Undercarriage Wear and Care Guide. USA: John Deere.

[9] Jones, D.A. 1992. Principles and Prevention of Corrosion. Macmillan.

[10] Indonesian Ministry of Public Works. 2012. Supply Chain Study of Construction's Heavy Equipments In Support of Infrastructure Investment. Executive Summary. Jakarta.

[11] Komatsu. 2009. Specification and Application Handbook. Edition 30. Komatsu: Japan.

[12] Maulana, I., Ibrahim, A., and Darmein, D. 2017. Analisa Kerusakan Komponen Undercarriage Excavator Hitachi Ex200 Pada Pt. Takabeya Perkasa Group Dengan Metode Fmea. Jurnal Mesin Sains Terapan. 1(1).

[13] Möller, H. 2006. The Corrosion Behaviour of Steel in Sea Water. The Shoutern African Institute of Mining and Metallurgy 8th. International Corrosion Conference.

[14] Ogoshi High Speed Universal Wear Testing Machine Instruction Manual.

[15] Prasetya, L., and Krisnaputra, R. 2014. Perancangan Special Tool Untuk Overhaul Undercarriage Backhoe Excavator Hitachi Ex 3600-6. Doctoral Dissertation. Universitas Gadjah Mada, Yogyakarta, Indonesia.

[16] Rochmanhadi, I. 1992. Alat-Alat Berat dan Penggunaannya. Yayasan Badan Penerbit Pekerjaan Umum, Jakarta.

[17] Rubinstein, D., and Coppock, J.L. 2007. A detailed single-link track model for multi-body dynamic simulation of crawlers. Journal of Terramechanics. 44(5): 355-364.

[18] Ryu, H.S.; Bae, D.S.; Choi, J.H.; and Shabana, A.A. 2000. A compliant track link model for high-speed, high-mobility tracked vehicles. International Journal for Numerical Methods in Engineering. 48(10): 1481-1502.

[19] Sarkar, A.D. 1980. Friction and Wear. Academic Press: London.

[20] Sunarya, Y. 2008. Mekanisme dan Efisiensi Inhibisi Sistein pada Korosi Baja Karbon dalam Larutan Elektrolit Jenuh Karbon Dioksida.

[21] Tretheway, K.R., and Chamberlain, J. 1991. Korosi Untuk Mahasiswa Dan Rekayasawan, Edisi Pertama, Pt. Gramedia Utama: Jakarta.

[22] United Tractors School. 2008. Product Knowledge Basic Course I. Jakarta Timur: Yayasan Karya Bakti United Tractors.

[23] Zum Gahr, K.H. 1987. Microstructure and Wear of Materials. Tribology Series. 132–148.

[24] Varun Kumar K and Mini K.M, Study on Corrosion Resistance in Concrete by Mineral Admixture Addition and FRP Wrapping of Reinforcement Bars. International Journal of Civil Engineering and Technology, 8(10), 2017, pp. 988– 1000.